MEASUREMENT OF ION BEAM LOSSES DUE TO BOUND-FREE PAIR PRODUCTION IN RHIC

J.M. Jowett, R. Bruce, S.S. Gilardoni, CERN, Geneva, Switzerland,
A, Drees, W. Fischer, S. Tepikian, BNL, Upton, NY, USA,
S.R. Klein, LBNL, Berkeley, CA, USA

Abstract

When the LHC operates as a Pb^{82+} ion collider, losses of Pb^{81+} ions, created through Bound-free Pair Production at the collision point, and localized in cold magnets, are expected to be a major luminosity limit. With Au^{79+} ions at RHIC, this effect is not a limitation because the Au^{78+} production rate is low, and the Au^{78+} beam produced is inside the momentum aperture. When RHIC collided Cu^{29+} ions, secondary beam production rates were lower still but the Cu^{28+} ions produced were predicted to be lost at a well-defined location, creating the opportunity for the first direct observation of BFPP effects in an ion collider. We report on measurements of localized beam losses due to BFPP with copper beams in RHIC and comparisons to predictions from tracking and Monte Carlo simulation.

INTRODUCTION

The electromagnetic interactions of colliding heavy ions, of atomic numbers Z_1, Z_2, produce copious amounts of e^+e^- pairs. In a small fraction of cases, the so-called bound-free pair production (BFPP) process,

$$Z_1 + Z_2 \rightarrow \left(Z_1 + e^-\right)_{1s_{1/2},\ldots} + e^+ + Z_2, \qquad (1)$$

the electron is created in a bound state of one ion. This results in a secondary beam of ions with altered magnetic rigidity emerging from the interaction point (IP).

At the LHC, which will collide lead ($^{208}Pb^{82+}$) nuclei, this hitherto unobserved beam-beam effect will be a major contribution to the luminosity decay [1,4]. In addition, the resulting $^{208}Pb^{81+}$ ions have a different magnetic rigidity, equivalent to a fractional deviation $\delta = 1/(Z-1)$, and follow a dispersive orbit $x_{\mathrm{BFPP}} = d_x(s)\delta$ as they emerge from the interaction point (IP). (Here $d_x(s)$ is the locally generated dispersion, not the periodic dispersion, $D_x(s)$). They are lost on the beam pipe as soon as the horizontal aperture satisfies $A_x = d_x(s)\delta$. At design luminosity, this is a 25 W beam impinging on a superconducting magnet. The quenching from the resulting heat deposition may limit the peak luminosity [3] and has been discussed in detail elsewhere [7,4,5,8].

As discussed in [2], the cross-sections for electron "capture" to each low-lying bound state have the approximate form

$$\sigma_{\mathrm{BFPP}} \approx Z_1^5 Z_2^2 \left[A \log \gamma_{CM} + B\right] \qquad (2)$$

where γ_{CM} corresponds to the ion energy in the centre-of-mass frame and A, B are constants. Comparing the future LHC with the present RHIC (Table 1) shows that the process is also significant for colliding gold nuclei. However although values of $d_x \approx 1.5$-2 m are comparable, the larger aperture, $A_x = 35$ mm compared to 22 mm in the LHC, means that the $^{197}Au^{78+}$ ions produced do not form a well-defined spot on the beam pipe. In addition the main cause of luminosity decay in current RHIC operation is intra-beam scattering rather than collisional effects.

Table 1: BFPP Cross sections, peak luminosity, BFPP rate and magnetic rigidity change at RHIC and LHC. Values are taken directly where possible, or estimated by fitting sums of contributions of the form (2), from the information in [2].

	σ_{BFPP} / barn	$L/10^{27}$ $\mathrm{cm^{-2}s^{-1}}$	BFPP rate /kHz	δ / %
LHC Pb-Pb 2750 A GeV	281	1	280	1.2
RHIC Au-Au 100 A GeV	114	1.5	170	1.3
RHIC Cu-Cu 100 A GeV	0.15	24	3.6	3.5
RHIC Cu-Cu 31 A GeV	0.08	1	0.08	3.5

During the Cu-Cu run of RHIC [6], δ *was* large enough (Table 1) for a spot to form and an opportunity arose to detect the lost Cu^{28+} ions from BFPP directly, even though predicted cross sections [2] and rates were very low. Loss monitors, in the form of PIN diodes (PDs), were installed in the Yellow Ring, downstream of the PHENIX experiment, around the location at the beginning of the arc where the BFPP spot was predicted to form and mounted on the magnet cryostats towards the exterior of the ring (where impacts were expected).

TRACKING FROM PHENIX IP

Tracking the BFPP ions in the ideal RHIC optics, using a method similar to the LHC studies [4,8], predicts that they will form a spot centred at $s = 135.5$ m from the IP at an incident angle of 2.7 mrad. If we instead take the real optics with orbit correctors, the impact point moves downstream to 136.4 m. There are also uncertainties in the orbit and impact conditions due to imperfect knowledge of magnet errors, initial orbit offset and angle at the IP and horizontal misalignment of the beam pipe at the impact point. Moreover some of the beam position monitors between the IP and the impact point were unreliable. An analysis of these sources of error, for which we do not have space here, indicates an uncertainty

in the impact point of the order of 2 m. Attempts to fit an orbit recorded during the measurements only changed the likely impact position by a few centimetres.

SHOWER SIMULATIONS

The shower in the magnet and the secondary particles coming out on the outside of the cryostat were simulated with the FLUKA 2005 Monte Carlo code [10,11] which uses DPMJET-III to simulate nuclear collisions. This code has been benchmarked by others against experimental data in the relevant energy range [9] and should be appropriate for the shower simulations. A 3D model of the geometry around the estimated impact point was built in FLUKA (see Fig. 1) and the initial conditions were taken from the optical tracking. A solid rectangular block of silicon was placed on each side of the cryostat along the magnets, as a continuous representation of the PDs, in order to study the longitudinal shape of the energy deposition. Fringe fields and magnet curvature were neglected.

According to the results shown in Figure 2, the maximum energy deposition in the silicon block outside the cryostat occurs at s=137.5 m where the shower has traversed the coils, yoke and cryostat. The distance in s between the average impact point and this maximum is approximately 1 m. Within another 1–1.5 m most of the shower has died out. As long as the impact point is located so that the shower is contained within the dipole, moving the impact point along s only translates the energy deposition profile in the silicon block. As the impact point approaches the end of the magnet, and more of the shower emerges into the void before the quadrupole, the profile changes qualitatively. A second peak appears at the entrance of the quadrupole and eventually exceeds the first one. Smaller angles of incidence cause the shower to go farther and the peak in the secondary magnet starts earlier.

The PD count rates were also estimated. Instead of the continuous bars, smaller silicon blocks of the same size as the PDs were implemented and positioned at the same spots on the cryostat. In the experiment, the PDs were first positioned in a wide configuration, 3 m apart. Later they were moved closer together, 0.5 m apart, around an observed maximum at 141.6 m. Both PD configurations were simulated, we can only show the wide configuration here (Table 2). This simulation has large error bars due to limited computer time and the result indicates only the order of magnitude to expect in the measurement.

COMPARISON WITH MEASUREMENTS

In the conditions of Fig. 3, in which PDs exhibit signals in clear temporal correlation with luminosity (also confirmed by Van der Meer scans and background analysis), the maximum signal is on the PD at 141.63 m . The count rates varied from 1-10 Hz at the maximum luminosity, depending on PD position. The order of magnitude of the count rates corresponds very well to the simulation (Fig. 3 and Table 2). However, the maximum

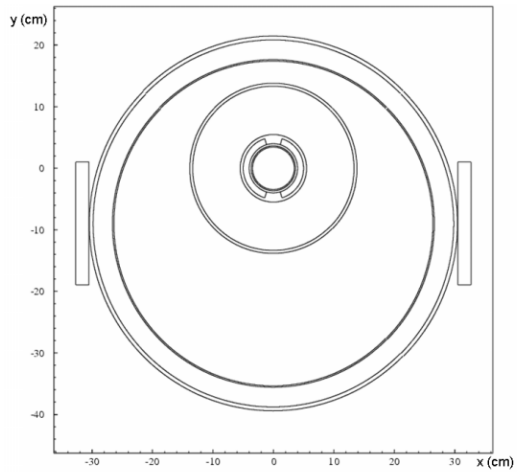

Figure 1 Cross section of FLUKA model of dipole, showing the silicon blocks on the outside of the cryostat used to model the PDs.

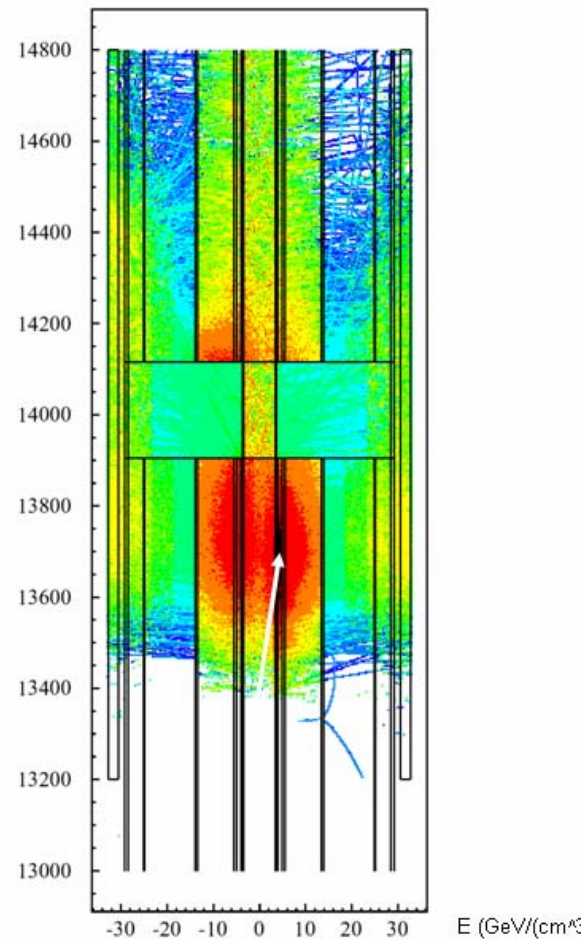

Figure 2: Energy deposition per ion (500 simulated) in a thick horizontal slice through the magnet in Figure 1. The white arrow indicates the impact on the beam pipe in the dipole, downstream of which a drift space and quadrupole can be seen. In the dipole, the correct field map was implemented inside the cold mass. It was sufficient to model the quadrupole as a copy of the dipole magnet but without magnetic field.

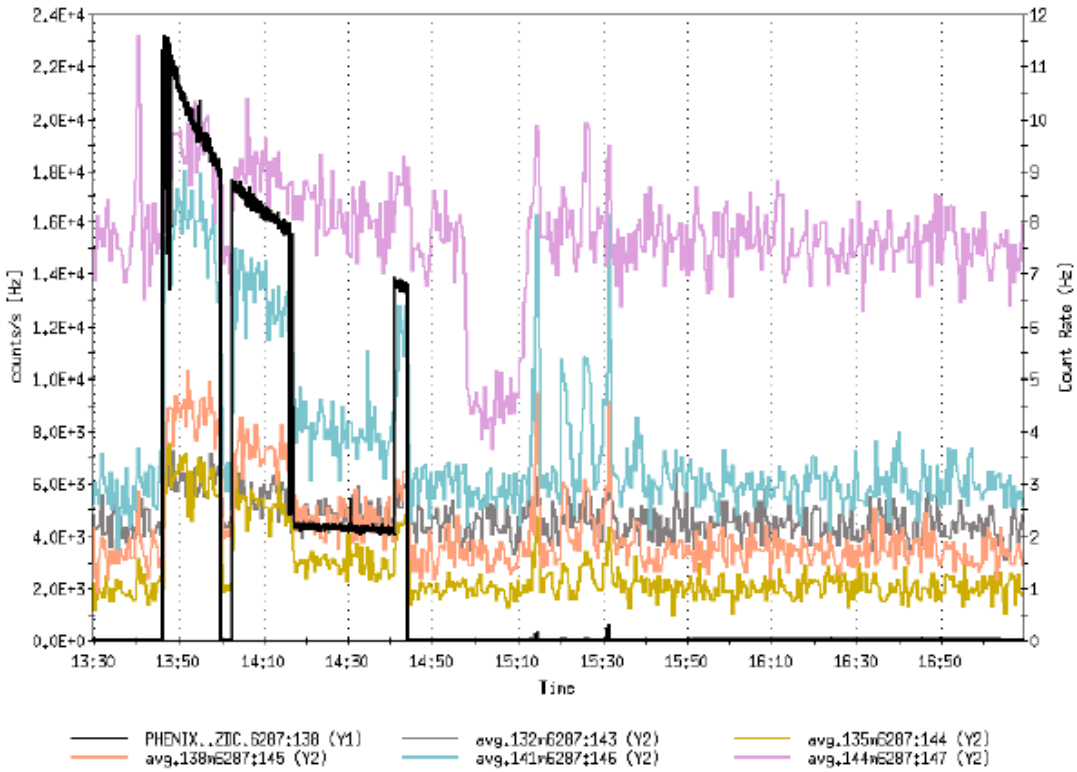

Figure 3: Count rates measured on the ZDC luminosity monitors (black, left scale) and PDs (colours, right scale) during a store in which beams were put into collision just after 13:45 with PDs in the wide configuration.

count in the simulation came from the PIN diode at 138.6 m, which does not exactly agree with the measurements. This means that, in reality, the second peak in the energy distribution outside the cryostat is actually higher than the first, while in the simulation the first peak is the higher. However, if the impact point is translated within the error bar, the simulated maximum moves further downstream and a good agreement with data can be found.

No signal was detectable in 31 A GeV operation, consistent with expectations.

Table 2 Simulated count rates in the PIN diodes, including the estimated PD efficiency of 0.3 counts/MIP and the sample standard deviation from 10 runs with 500 particles in each, normalised to the luminosity (9.1×10^{27} $cm^{-2}s^{-1}$) corresponding to the peak in Fig. 3.

Wide Configuration		
Position s [m]	Count [Hz]	σ
132.6	0	0
135.6	2.1	1.3
138.6	16	2.5
141.6	11.8	8.5
144.6	1	0.4

CONCLUSIONS

Within the uncertainties associated with the experimental conditions and the simulation of the ion showers, these data are consistent with the signal expected from Bound-Free Pair Production in the collisions of Cu ions at the RHIC interaction point. We intend to publish and analyse further data in more detail elsewhere. As such, they constitute the first detection of this effect in an ion collider and a valuable test of our ability to quantitatively predict it for the LHC.

Acknowledgments: We thank A.J. Baltz, R. Gupta, K. Hencken, T. Roser for help and fruitful discussions.

REFERENCES

[1] A.J. Baltz et al, Phys. Rev. **E 54** 4233 (1996).
[2] H. Meier et al, Phys. Rev. **A 63** 032713 (2001)
[3] S.R. Klein, Nucl. Inst. & Methods **A459** 51 (2001).
[4] J.M. Jowett, et al, EPAC2004, MOPLT020 and references therein.
[5] J.M. Jowett, et al, PAC2005, TPAP012.
[6] F. Pilat et al, PAC2005, TPAT093.
[7] The LHC Design Report, Vol. I The LHC Main Ring, CERN-2004-003 Chapter 21 and references therein.
[8] R. Bruce et al, CERN LHC Project Note 379 (2006).
[9] S. Roesler, R. Engel, J. Ranft, hep-ph/0012252
[10] A. Fasso et al, CERN-2005-10.
[11] A. Fasso et al, arXiv:hep-ph/0306267 (2003)